

Lessons Learned in the Operation of the HIBARI: Variable Shape Satellite

Daiki Kobayashi, Kei Watanabe, Hiroyuki Kobayashi, Yuki Amaki, Kenichiro Takahashi, Yusaku Ozeki, Katsuki Tashiro, Riku Nishio, Ryo Saito, Yusei Kawaguchi, Kiyona Miyamoto, Toshihiro Chujo, Hiroki Nakanishi, Yoichi Yatsu, Saburo Matunaga
Tokyo Institute of Technology,
554, Ishikawadai 1st Bldg., 2-12-1, Ookayama, Meguro, Tokyo, 152-8552, Japan, 81 3 5734 2609
kobayashi.d.an@m.titech.ac.jp

ABSTRACT

We have developed the 50 kg microsatellite “HIBARI”. The satellite demonstrated a novel attitude control method called “Variable Shape Attitude Control (VSAC)”. VSAC is a method that can quickly control attitude and has low energy consumption using reaction torque by driving variable shape structures. HIBARI was launched in 2021 under the Innovative Satellite Technology Demonstration Program led by JAXA. We have been operating the satellite for two years and have demonstrated the VSAC mission. We achieved all minimum and full success criteria, including 30 deg/10sec agile attitude change.

On the other hand, we experienced problems like the degradation of satellite components and other problems that could not be confirmed by ground tests. There was degradation of the paddle drive unit and influence of the paddles on bus components, which are unique to variable shape satellites. In addition, there was a case in which a paddle collided with the satellite structure due to an operational error. After the collision, the satellite’s integrity was evaluated by taking images of the paddle with the onboard camera and checking the telemetry data before and after the collision. During more than two years of operation, we have obtained knowledge about possible failures and countermeasures for satellites with variable shape structures.

INTRODUCTION

In recent years, microsatellites have attracted attention due to the advantage of low cost and short development time. Accordingly, mission requirements for microsatellites have become more advanced, such as Earth/astronomical observations, and constellations. However, microsatellites have technical limitations, such as volume, mass, and power. To solve this problem, onboard devices need to be smaller and more multifunctional.

To meet these needs, our team proposed Variable Shape Attitude Control (VSAC). This is a novel attitude control method that can control the attitude and orbit by driving satellite structures. Our team has developed “HIBARI” to demonstrate this method in orbit^{1,2,3}. The satellite was developed and launched in November 2021 under JAXA’s Innovative Satellite Technology Demonstration Program. We have been operating this satellite for two years⁴.

VARIABLE SHAPE FUNCTION

The variable shape function mainly achieves the following functions by changing the system shape.

- (1) Agile attitude control using reaction torque by changing the satellite shape based on multi-body dynamics^{5,6}.
- (2) Orbit/Attitude control using external forces, such as air drag forces and solar radiation pressure, by changing the satellite’s cross-sectional area.
- (3) Changing the satellite function to suit a mission by changing the shape of the satellite.

Figure 1 illustrates the concept of variable-shaped attitude control (VSAC) as described in (1). This method enables the satellite to change its body attitude using reaction torque by driving satellite structures, such as solar array paddles. The proposed method drives the motor only when the attitude is controlled. Therefore, it is more energy efficient than conventional CMGs which must rotate wheels constantly. In addition, the angle of attitude change can be increased by increasing the inertia of the driving structures. This increase contributes to higher attitude stability. VSAC enables satellites to engage in agile attitude change and stabilize attitudes. Also, VSAC enables satellites to change the 3-axis attitude by using control under non-holonomic constraints.

Figure 2 illustrates the concept of orbit/attitude control described in (2). The satellites are affected by external forces like air-drag force and solar radiation pressure in orbit. The magnitude of these forces can be changed by changing the satellite's cross-sectional area. By changing its shape and attitude, the satellite controls external force. This leads to control of the satellite's orbit/attitude.

In terms of (3), for example, satellites can control power supply from solar array paddles by changing solar cell direction from the sun. Also, this enables satellites to control thermal coupling parameters by changing satellite shape. Also, it's possible to change observation modes by changing observation devices like the interferometer.

In HIBARI, we realized multifunctional actuators by using solar array paddles as driving structures. These solar array paddles contribute to agile attitude control, high attitude stability, and power generation.

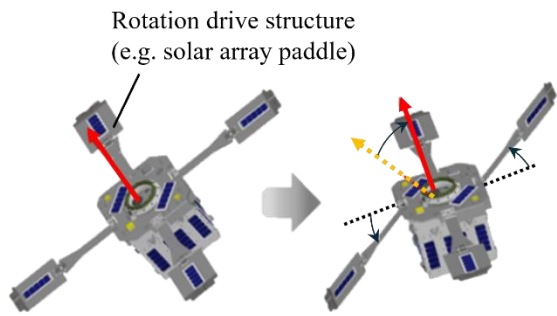


Fig 1. Concept of VSAC

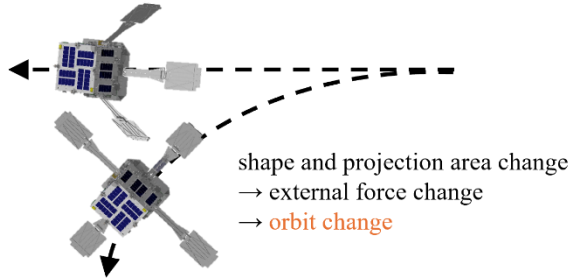


Fig 2. Concept of orbit control using external forces

HIBARI MISSION AND SYSTEM

Mission Design

We set success criteria as shown in Table 1. For minimum success, to confirm the attitude change predicted by variable shape function of the motor drive. For full success, agile attitude changes (15deg/10sec: equivalent to CMG for microsattellites) by VSAC. For extra success, agile attitude change (30deg/10sec), large

attitude change (40deg) using non-holonomic constraints, and attitude stability (300arcsec/1sec) cooperate with RW. In addition, orbit/attitude control using air-drag force is under demonstration as an extended operation.

Table 1 success criteria

| Level | Mission | achievement |
|-------|---|-------------|
| Min, | Confirm attitude change predicted by variable shape function of motor drive | ○ |
| Full | VSAC • Agility:15 deg/10 sec Pointing Accuracy:5 deg | ○ |
| Extra | VSAC • Agility: 30 deg/10 sec • Stability: 300 arcsec/1 sec | ○ |
| | • Large-Angle Maneuver using Non-Holonomic Control: 40 deg Corporative control with RW • Stability: 300 arcsec/10 sec Confirmation of orbit/attitude change with controlled atmospheric resistance | ongoing |

System Design

Table 2 lists HIBARI's system specifications. HIBARI is a 50kg class satellite. The size is $570 \times 570 \times 550 \text{mm}^3$ and mass of the bus system is 45kg, and each solar array paddle is 2.5kg. Figure 3 shows the satellite configuration. HIBARI stowed its paddles during launch and deployed them after being injected into space. Because HIBARI uses reaction torque when driving paddles, we designed the solar array paddles to have a larger moment of inertia. This requirement was met by adding weight to the paddles. As a result, we achieved a high moment of inertia after deploying paddles as shown below.

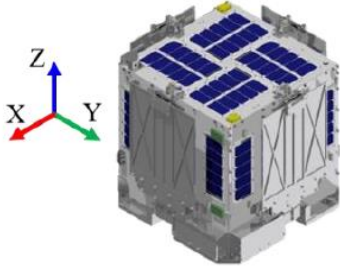
$$I_{stowed} = \begin{bmatrix} 3.25 & -7.93 \times 10^{-3} & 1.00 \times 10^{-4} \\ \text{Sym.} & 3.25 & 1.00 \times 10^{-4} \\ & & 3.30 \end{bmatrix} \text{kgm}^2$$

$$I_{deploy} = \begin{bmatrix} 7.08 & -7.93 \times 10^{-3} & 9.59 \times 10^{-4} \\ \text{Sym.} & 7.08 & 6.09 \times 10^{-4} \\ & & 11.1 \end{bmatrix} \text{kgm}^2$$

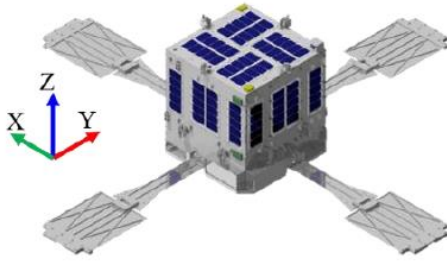
Table 2 System specifications

| | |
|------|--|
| Size | $570 \times 570 \times 550 \text{mm}^3$ (Paddle Stowed) |
| Mass | 55 kg (Bus 45 kg, Paddle 2.5 kg \times 4) |
| Comm | S-band Tx/Rx ANT \times 2 (DL 10kbps ~ 1Mbps, UL:1kbps) |

| | |
|-------|--|
| | Global Star Tx ANT (100kbps) |
| Power | Li-ion Battery 161Wh Nominal generated power when pointing : 40W |
| Orbit | Sun-synchronous orbit (perigees altitude 547km, apogee altitude 565km, orbital node local solar time 9:30) |



(a) Paddle Stowed Configuration



(b) Paddle Deployed Configuration

Fig 3. HIBARI appearance

OPERATION RESULT

Agile attitude control

HIBARI demonstrated a Variable Shape Attitude Control system via a paddle drive experiment for two years⁷. We achieved the VSAC mission's minimum, full, and one of extra. Figure 4 illustrates the agile attitude change using paddles. This shows the angle of attitude change by 3-2-1 Euler angle. The result shows that the satellite attitude rotates along the y-axis approximately 35 degrees in 10 seconds when driving paddles. We set the maximum paddle velocity to 10 deg/s, and maximum acceleration to 5deg/s², and drive opposing paddles up to ± 80 degrees.

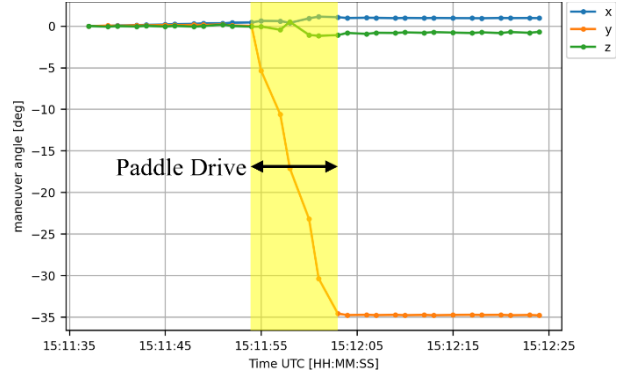


Fig 4. attitude change by driving paddles.

Attitude control using non-holonomic constraints

We demonstrated attitude changes using non-holonomic constraints. We evaluated the attitude change by sequentially driving paddles. We set the maximum paddle velocity to 10deg/s, and maximum acceleration to 8deg/s².

1. Drive -X paddle to 80 degrees
2. Drive -Y paddle to 80 degrees
3. Drive -X paddle to 0 degrees
4. Drive -Y paddle to 0 degrees

Figure 5 shows the attitude change results using 3-2-1 Euler angle. It shows that all axes rotate 5 degrees during the paddle drive process under non-holonomic constraints. It was confirmed that VSAC can change its attitude around the z-axis, which cannot be achieved by driving only X or Y paddles.

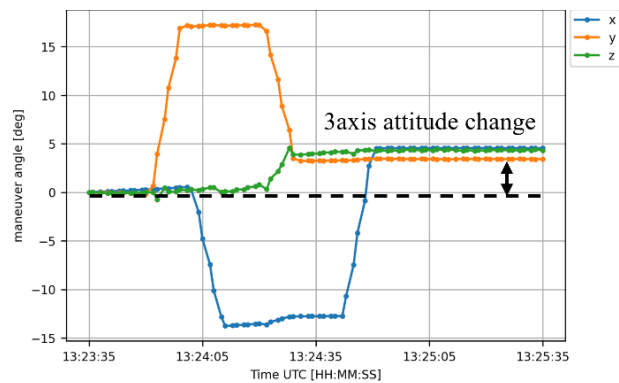


Fig 5. Attitude change using nonholonomic-constraints

During the two years of operation, we experienced problems such as deterioration of satellite components and problems that were not be confirmed on ground tests. For example, radiation degradation, degradation of the

paddle drive unit, and influence of the paddles on bus components, which are unique to variable shape satellites. These degradations will be discussed in the following sections.

FAILURE CAUSED BY SPACE ENVIRONMENT

Failure of gyroscope

There were anomalous values from the STIM210 gyroscope on 2023-06-16 at 12:42:56. There were anomalous values on the x-axis temperature telemetry, and the x-axis temperature value changed randomly up to $\pm 126^\circ\text{C}$ as shown in Figure 6 and the angular speed value changed to 0.

To investigate the cause, we checked satellite telemetry. First, we verified the y-axis and z-axis values, which appeared to be correct. Therefore, we suspect that the anomalous data were not caused by communication errors from the satellite onboard computer. Second, we considered degradation due to Total ionizing dose (TID). When anomalous output occurred, HIBARI was operated for 1.5 years. We estimated the total radiation dose altitude of 500 km is 1 to 2 krad/year, so we assumed TID was about 1.5 to 3 krad. Based on the radiation test data⁸, STIM210 can endure up to 5 krad under power on. Thus, we assumed that degradation by TID is unlikely. Third, we evaluated the possibility of a Single Event Effect (SEE). However, there was no over-current detection or suspicious current changes. Additionally, it did not resolve after resetting the sensor. Therefore, it does not appear to be a typical SEE phenomenon. Nevertheless, we analyzed satellite position data at the time of anomalous data output. Figure 7 shows the position where the gyroscope first outputs anomalous values. The anomaly occurred within the South Atlantic Anomaly. Therefore, we suspect that these anomalous data were caused by a Single Event Effect.

We also considered the reason for the anomalous output from the thermal telemetry and angular velocity telemetry. The angular velocity telemetry is calibrated by temperature data, so degradation in the temperature measurement device affected the angular velocity telemetry. We considered the effect of STIM210 failure. During normal operation, HIBARI controls satellite attitude using another coarse gyroscope. So, there was no critical error on the satellite. However, it became more difficult to execute mission operations using STIM210.

As a countermeasure, we changed the reset cycle from once a week to twice a week. In addition, for the next developing satellite, we will equip two STIM210 gyroscopes for redundancy and prepare a radiation shield.

We designed harnesses that supply power to each STIM210 and share a communication line. We verified the data received from each sensor. Furthermore, we designed an aluminum box with a thickness of 5 mm as a radiation shield under consideration of radiation resistance and processibility. We aim to suppress radiation exposure. It decreases TID and the number of SEE and extends the satellite lifespan.

On 2024-02-08 at 13:40:47, STIM210's x-axis thermal and angular velocity telemetry became consistent with the other two axes on. We conclude that STIM210 has recovered. The reason for recovery is being investigated. We speculate it returned to normal due to the radiation effect.

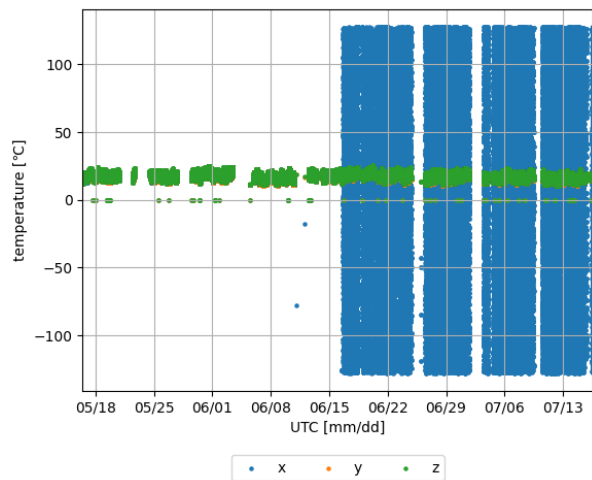


Fig 6. Thermal telemetry of STIM210

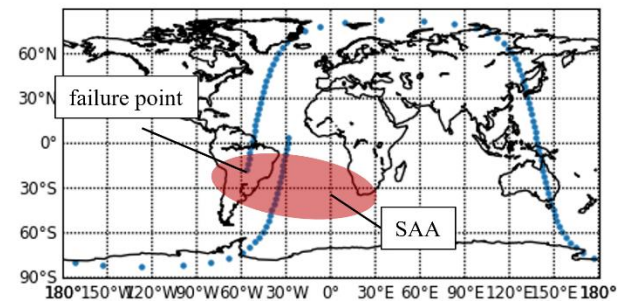


Fig 7. Anomalous output position of STIM210

FAILURE OF BUS SYSTEM UNIQUE TO VARIABLE SHAPE SATELLITE

Next, we faced at bus system failure unique to Variable Shape Satellite.

Degradation of absolute encoder on solar array paddles

There are 4 drivable paddles on the HIBARI, and each paddle is equipped with an absolute encoder to measure the paddle angle. We verified the anomalous value of the absolute encoder on the +Y solar array paddle on 2022-10-13 at 12:52:35. Despite not sending commands to actuate the paddle, the absolute encoder value changed to 26.19 degrees, as shown in Figure 8. We concluded that the actual paddle angle did not change, based on the data from the other relative encoder in the motor and satellite attitude.

To investigate the cause, we examined the satellite telemetry. We found no discernible difference in current just before and after the incident. However, there was the current flow change of 4-paddle's absolute encoder 4 months before the anomalous value. Figure 9 shows that approximately 1.5 times the steady current flows to the +Y absolute encoder, and thereafter, the steady flow decreased. We have designed the current hardware and software over-current protection system in the satellite before launch. However, we set a high threshold of over-current protection due to the fear of missed detection of over-current. Thus, we assume the over-current protection didn't work because the over-current flows under the threshold of hardware and software over-current protection. In addition, the absolute encoder was equipped in a severe radiation environment. Figure 10 shows the detailed view of the gearbox. The gearbox, which consists of a motor and an absolute encoder, was equipped outside of the satellite, so as not paddles to collide with the satellite bus. The thickness of the gearbox cover was designed 1 mm aluminum. This was not enough to shield radiation. Now, we turn on the absolute encoder only when sensing the paddle angle and nominally turn it off as a countermeasure to Single Event latch-up.

As a countermeasure, a suitable threshold parameter should be set based on orbit data after transitioning to the steady operation phase. In addition, variable shape satellites require higher radiation resistance, because they often operate drive structures outside the satellite, which is equipped with drive mechanisms and angle sensors. Therefore, to develop the next variable shape satellite, we consider using a high resistance angle sensor such as resolvers.

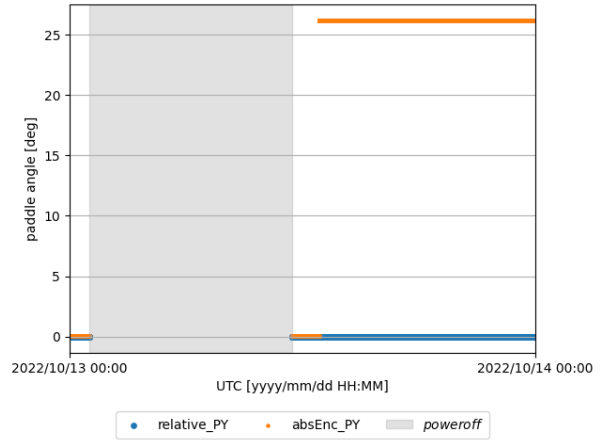


Fig 8. Anomalous value of absolute encoder

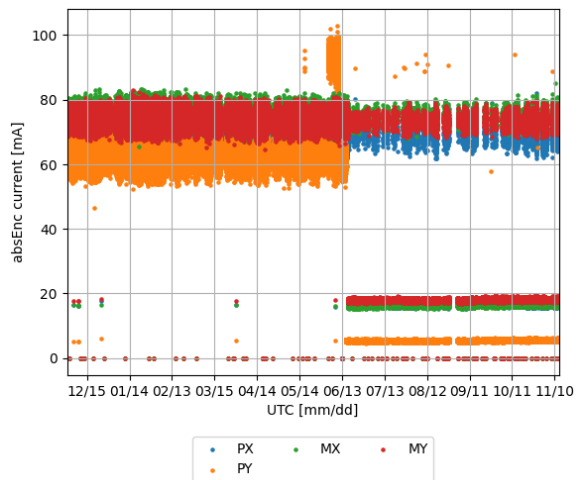


Fig 9. Current of absolute encoder

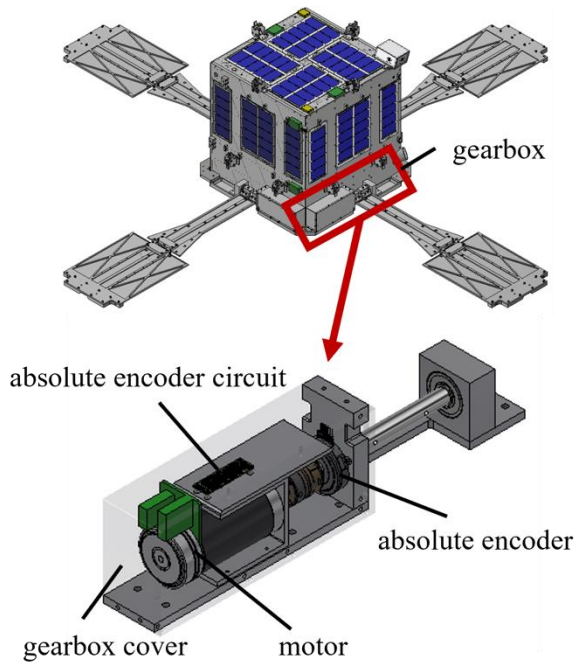


Fig 10. Detail of gearbox

Power supply of solar cell on drivable solar array paddle

HIBARI achieved agile attitude control by driving solar array paddle and also generates power from solar cells. Figure 11 shows the HIBARI solar cell on solar array paddles at the -Z side. These solar cells demonstrated multifunctionality in terms of variable shape function contributing to both agile attitude control and power supply. Each paddle is equipped with 5 series of solar cells. These cell's voltage and current were recorded, and the power supply was calculated. Figure 12 shows the arrangement of solar cells on solar array paddles. The same color cells are connected in parallel. Figure 13 shows the extracted system diagram of the solar cells. There are 5 current/voltage measurement points labeled with numbers.

We verified the power supply effect of solar cells in solar array paddles. As a premise, the EPS system of HIBARI controls power charging by switching constant voltage (CV) and constant current (CC) control. The system decreases the power supply near full charging using CV control. In addition, this satellite is set to point the +Z side to the sun's direction, so the -Z side rarely points sun's direction. Based on this premise, we selected an analysis period when solar cells can generate enough power. We selected 24 hours from 2022-1-6 22:00. Figure 14 shows each solar cell on solar array paddle current. All solar cell current is under 125 mA. We

confirmed that current flows approximately 500 mA by experimenting with current-voltage characteristics on the ground before launch, however, current flows in orbit were low compared to ground tests. In addition, current flows should change depending on the sun angle, but the output is almost constant. In addition, current flows are recorded in shade.

To investigate the cause, we analyzed measurement points 3 and 5 in Figure 13. Figures 15 and 16 show these point's current and voltage. We assumed power generation from albedo in the shade, however, there was almost zero current flow and voltage in the shade. This suggests there is no power generation in the shade. In sunshine, the power generation should be near 500 mA at 5 series of solar cells on the solar array paddle. So, we checked the current/voltage measurement circuit of measurement point 1 and 2. Figure 17 shows the current/voltage measurement circuit of measurement point 1,2. This circuit measures current and voltage using solar cell voltage. Thus, it cannot measure correct data under there is no solar cell power supply. Also, the voltage measure point V_{sens} was arranged after the ideal diode. So, this circuit measures the voltage after maximum power point tracking control (MPPT control) at MPPT converter shown in Figure 13. It also controls the BOTTOM_PXPY cell. Thus, this cannot measure the voltage of the solar cell on a solar array paddle only. This makes it difficult to distinguish the cause of the low current flow of solar cells. It was necessary to design the current/voltage measurement point before the ideal diode could be used to analyze the solar cell output.

The reason why low power generation of solar cells on solar array paddles is assumed that the current-voltage characteristic of solar cells was changed by the thermal environment or cracking in launch vibration. These lead to a decrease in open circuit voltage. MPPT control also optimize the Bottom_PXPY cell power, which is mounted on a satellite bus, so the generated voltage may exceed the open circuit voltage of the solar array paddle cell and power generation became low.

As a lesson, the thermal environment of variable shape satellites changes depending on the shape, and this leads to the deterioration of power generation efficiency because MPPT control tracks irregular current-voltage characteristics of solar cells. To solve this, each drivable solar array paddle cell should input the power control unit separately. In this way, we must consider changes in the thermal environment or current-voltage characteristics depending on shape change to design solar cell configuration.

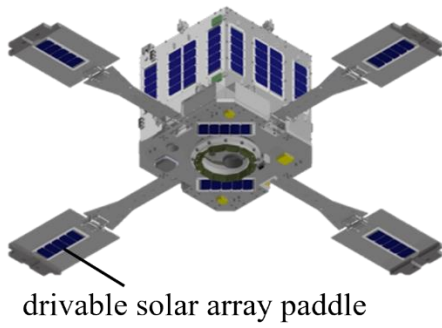


Fig 11. solar cell paddle cells of HIBARI

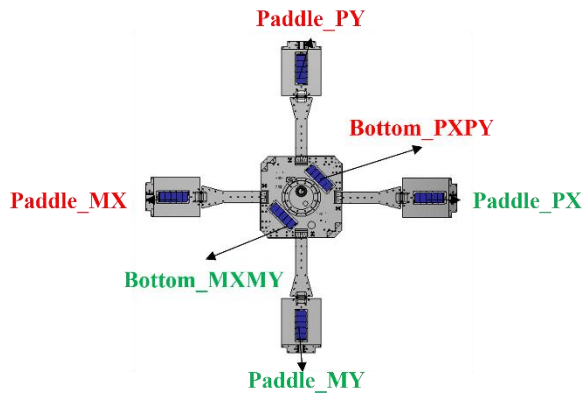


Fig 12. HIBARI MZ side arrangement of solar cell

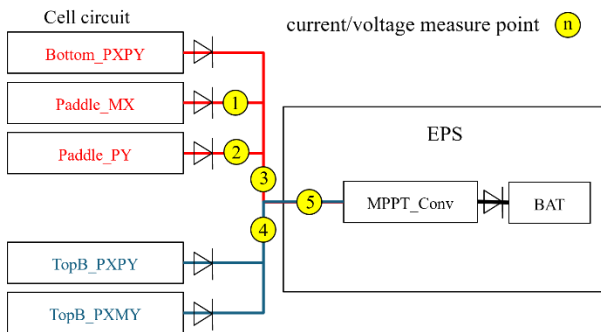


Fig 13. EPS system diagram (extracted)

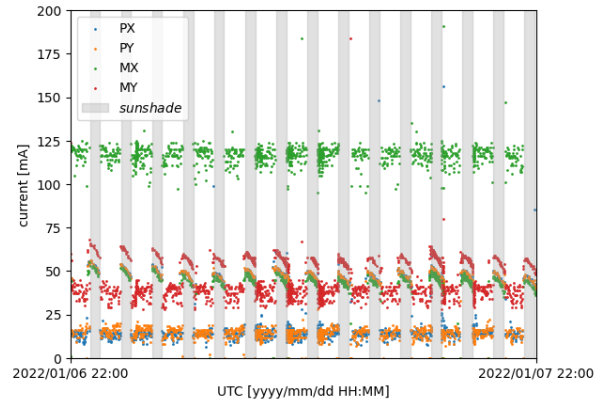
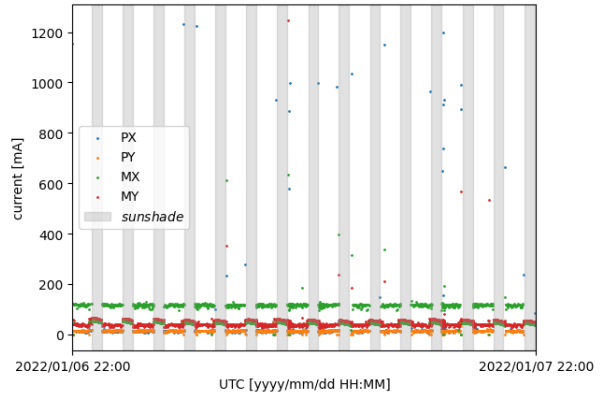


Fig14. Solar array paddle cells current (upper: all data, lower: expand under 200 mA)

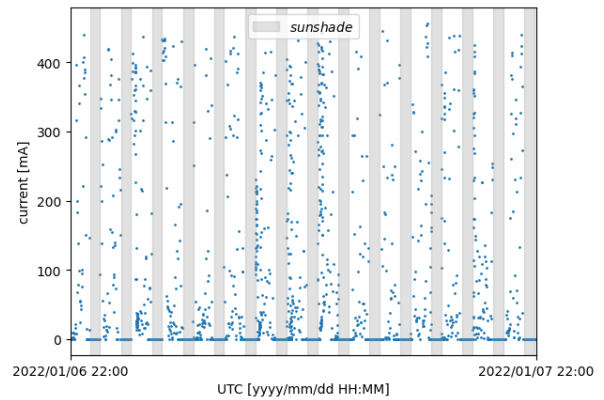


Fig15. Current value of measure point 3 in Fig13

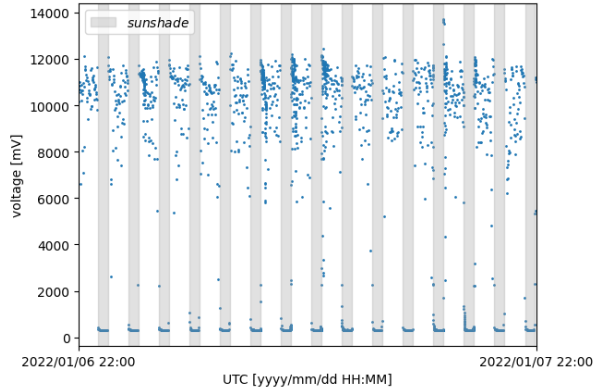


Fig16. Voltage value of measure point 5 in Fig13

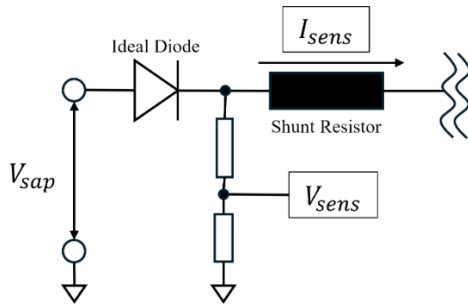


Fig17. Measurement circuit of paddle solar cell

Influence of drivable structure on bus system

There is the possibility of interference due to drivable structures by changing satellite shape. For example, sun sensors equipped with HIBARI have 170 degrees wide field of view. This often interferes with solar array paddles. We analyzed the satellite telemetry in Figure 18 shape. Figure 18 shows the interference area as red color. We compared the sun's direction output between SAS_PZ and SAS_MX. There was a large error of up to 175 degrees as shown in Figure 19. We verified sun reflection light was detected before launch, so we assumed these errors were caused by reflected light from satellite structures.

As a countermeasure, we arranged sensors that rarely interfered with the structure. In addition, we selected sensor data that rarely interfered with structures. For example, a +Z side sun sensor is selected when the paddle angle is 0 deg. However, it is difficult to arrange sensors that never interfere with the structure. Therefore, we need to develop the method to select sensor data, sensor arrangement, and satellite shape design.

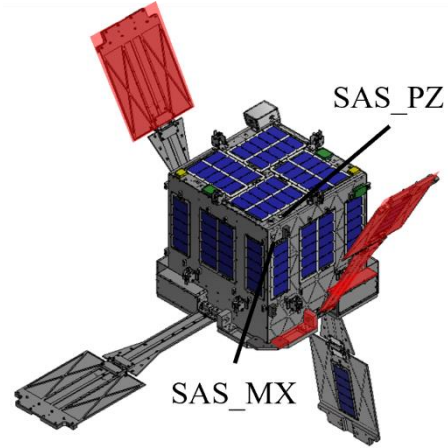


Fig18. interference area

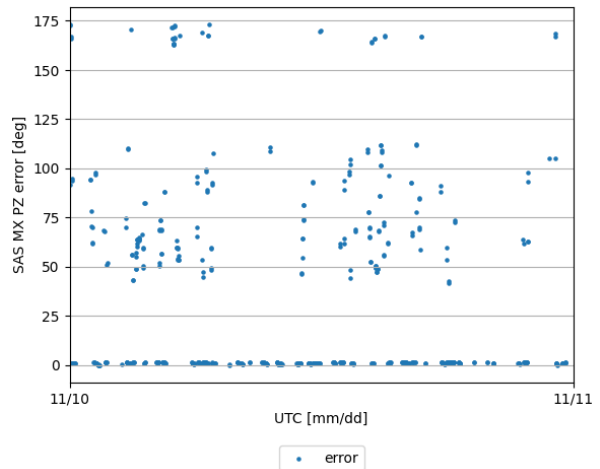


Fig19. sun direction error between SAS_PZ, SAS_MX

PADDLE MISS DRIVE AND RECOVERY

We sent an endianness missed command when experimenting paddle drive on 2023-11-22. HIBARI executed a command which drove the paddle over the designed value, ± 80 degrees. However, the limit switch of the paddle drive unit reacted and stopped the paddle at -88.9 degrees. Figure 20 shows miss driven shape.

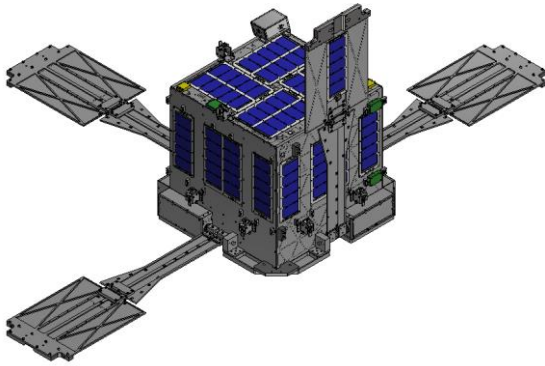


Fig 20. paddle miss drive shape (MX : -88.9 deg)

Correspondence to miss driving

First, shoot a paddle image to understand the paddle situation. Figure 21 shows paddle images. The left image shows the paddle exterior before deploying the paddles. The right image shows the paddle exterior after miss driven. There was no fatal degradation of the paddle in the image.

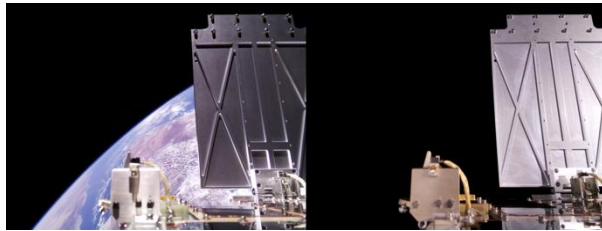


Fig21. paddle image
(Left: before paddle deploy,
Right: after miss driven)

Second, we analyzed to confirm there was no problem before and after the missed drive. We analyzed solar cell power generation and confirmed that there was no fatal decrease. But there was a bit decrease in power generation caused by the shade of miss driven MX paddle. Figure 22 shows satellite MX side solar cell power generation. This shows power generation decreased by 5W, but it was not a problem to operate the satellite.

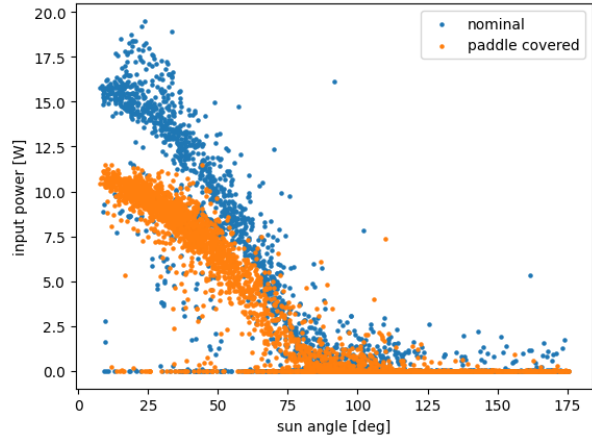


Figure 22. MX side power generation covered with solar array paddle

Assumption of satellite status from images and telemetry

As mentioned above, no fatal effects were observed on the satellite bus system. Thus, we analyzed paddle images and mission telemetry to confirm the paddle status after the missed drive. First, we confirmed the structural change caused by paddle collision at paddle hold mechanism from the difference in Figure 21. Therefore, we checked paddle collision analysis using satellite CAD and EM models.

Figure 23 shows the appearance of the hold mechanism, and Figure 24 shows the mechanism of the hold mechanism. This structure consists of a link part and a hemisphere pin. It holds the paddle by pushing the hemisphere pin into the paddle structure. We use string tension to push the hemisphere pin. The hemisphere pin gets out when string tension is released by fusing wire.

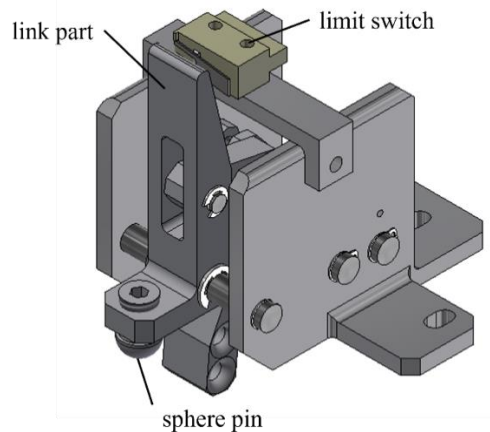


Fig 23 appearance of hold mechanism

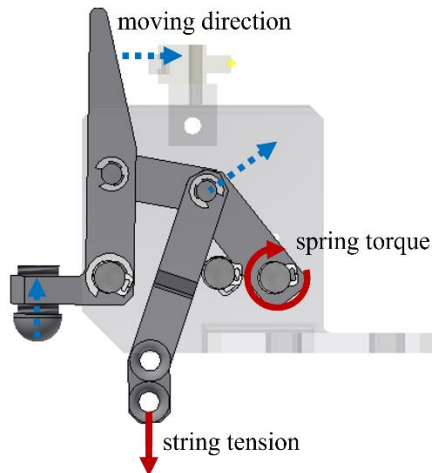


Fig 24. mechanism of hold mechanism

Figures 25 and 26 show that the link part moves by a colliding paddle caused by driving the paddle over the designed limit. From this analysis, we confirmed the link mechanism moves by colliding the paddle from the CAD and EM models.

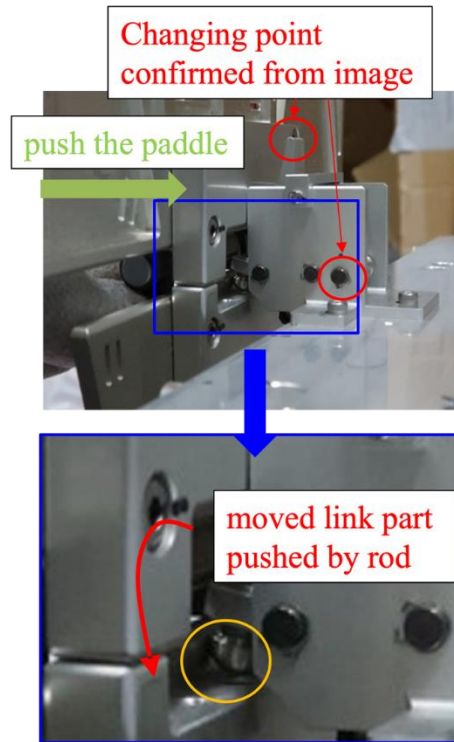


Fig26. Paddle collision analysis using EM model

Next, we analyzed the effect of collision on satellite telemetry. Figure 27 shows the absolute encoder value and relative incremental encoder value. There was a 12.6-degree difference. Figure 28 shows that the gearbox is equipped with a limit switch and paddle hold parts. Figure 29 shows the detail of the gearbox. There are motor shaft and paddle shaft. These two shafts are connected by coupling to absorb assembly errors. From this mechanism, the absolute encoder measures the paddle angle, incremental encoder measures the motor rotation angle. Thus, each encoder measures the angle between couplings. Thus, the difference between the encoders values is caused before and after coupling. The limit switch is designed to stop the paddle when driving the paddle over the designed angle. However, it's possible to drive the paddle over designed limit angle because of communication delay or paddle inertial force.

Changing link parts point confirmed from image

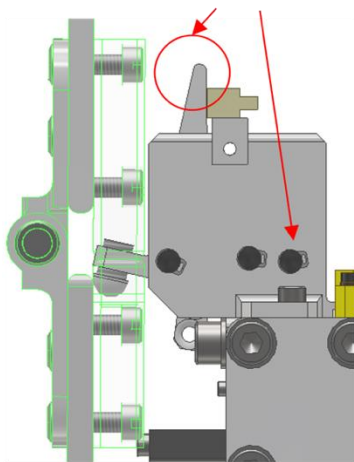


Fig25. Collision analysis using CAD model

To investigate this error, we confirmed using Tablesat. Figure 30 shows the coupling condition after driving up to collide to limit switch. From this experiment, we confirmed that there is a difference between the paddle shaft angle and the coupling rotation angle. This is assumed that the coupling shifted by the torque loaded by rotation of the motor after the collision. In addition, this shift is approximately 12.2 degrees, like the difference between the absolute encoder and the incremental encoder of orbit data. Thus, we assumed coupling shift had occurred in orbit.

We considered the impact of this error on the paddle drive experiment. This error was caused by a rotating motor shaft angle larger than the paddle shaft. However, the satellite controls the paddle angle using the absolute encoder value, which measures the paddle shaft angle directly. In addition, the incremental encoder error value could be reset by power off. Thus, we conclude that there is no effect on the paddle drive experiment.

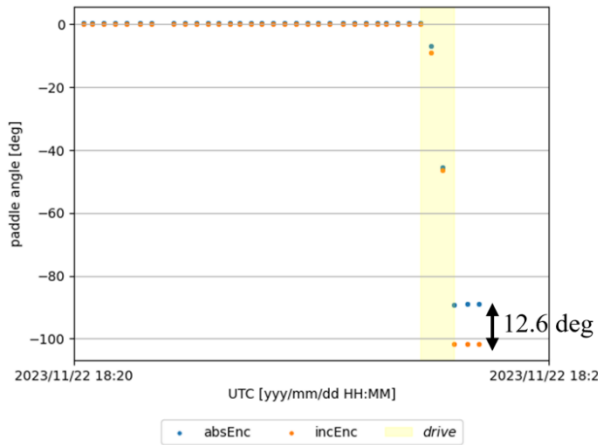


Fig27. Absolute encoder and incremental encoder value when paddle collided

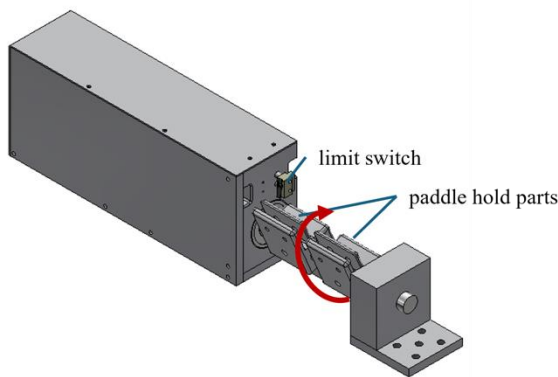


Fig 28. Appearance of gearbox

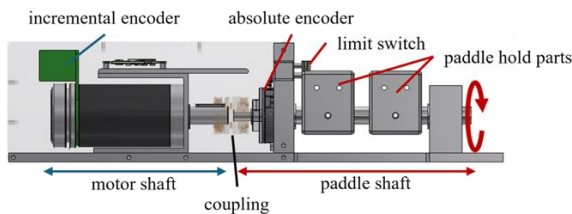
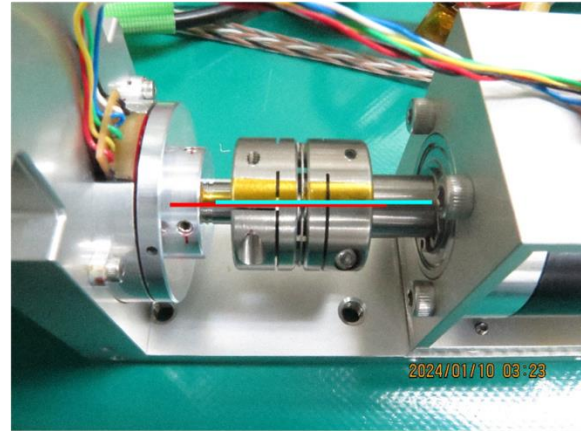
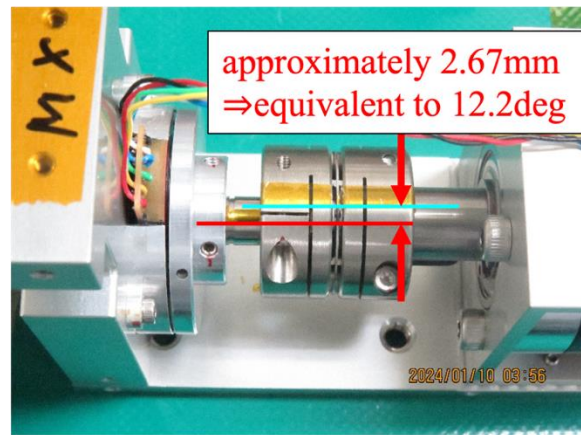


Fig 29. Detail of gearbox



Before collision



After collision

Fig 30. Coupling situation when paddle collided

Paddle recovery operation

As above, we replicated the phenomena of paddle collision. We confirmed that there was no fatal degradation on the satellite. After that, we drove the paddle to 0 degrees. To prepare for the anomalous situations, we conducted paddle recovery operations in real-time and took images while driving paddles from -88.9 degrees to -80 degrees. We conducted a paddle recovery operation on the pass of Tohoku University to monitor the satellite in real-time.

We shoot camera to know the paddle situation, so we need to avoid the backlight of the sun. But it is difficult to realize this need because the HIBARI paddle drive mode stops RW. This leads to an exchange of angular momentum between RW and satellite and rotates the satellite attitude. So, we set conditions that avoid the sun backlight under the exchange of angular momentum. We set the satellite point direction and RW angular velocity.

We set conditions from camera direction, RW momentum of inertia, and the sun pointing stability.

- ① The angle between satellite +Z side direction and sun direction is under 15.6 degrees.
- ② Angular velocity of all RWs are under 4000 rpm.
- ③ Drive a paddle at the pass of Tohoku University to monitor satellite data.

To realize these conditions, we confirmed feasibility by pre-experiment using HIBARI sun point fine mode. HIBARI's sun point fine mode uses RW to realize 2-axis sun pointing. However, this mode cannot control RW saturation. So, consider about unloading time using magnetic torquer (MTQ), shoot the camera 1 hour after starting controlling. Figures 31 and 32 show the results. These results show the paddle recovery condition was realized.

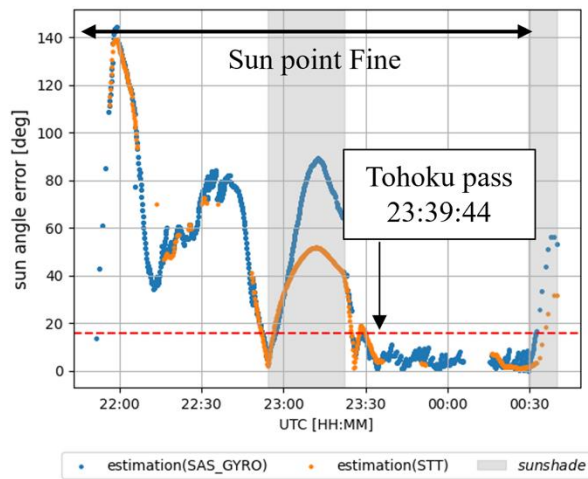


Fig 31. Sun angle error while pre-paddle recovery operation

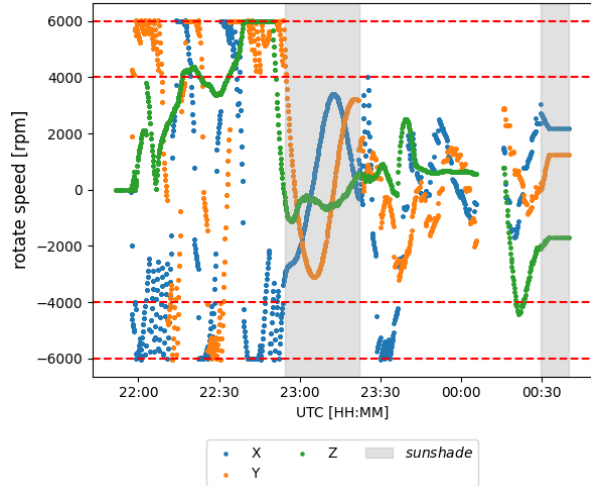


Fig 32. RW angular velocity while pre-paddle recovery operation

Result of paddle recovery operation

We conducted a paddle recovery operation on 2024-04-01 at 22:56:42. At this time, the sun angle error was 6.4 degrees, RWs angular velocity was 0 rpm: x-axis, 2033 rpm: y-axis, 2149 rpm: z-axis. Figures 33, 34, and 35 show the result of the paddle drive. We took images while driving the paddle from -88.9 degrees to -80 degrees. Figure 33 shows images while driving a paddle. Figure 34 shows the sun angle history, Figure 35 shows the paddle angle while paddle driving. Sun angle condition, under 15.6 degrees was realized all the time. However, the paddle angle difference between the absolute encoder and the incremental encoder was 0.46 degrees. We checked past paddle drive experiments, there was about a 0.5-degree difference. We assume the count error of the encoder or the rattle of the paddle drive unit.

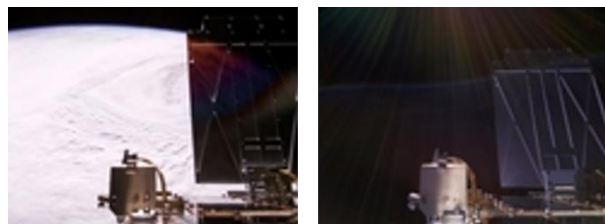


Fig 33. Paddle recovery image (Left: before driving, Right: after driving)

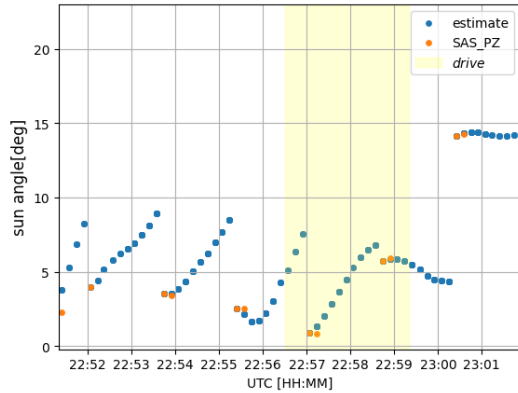


Fig 34. Sun angle while paddle recovery

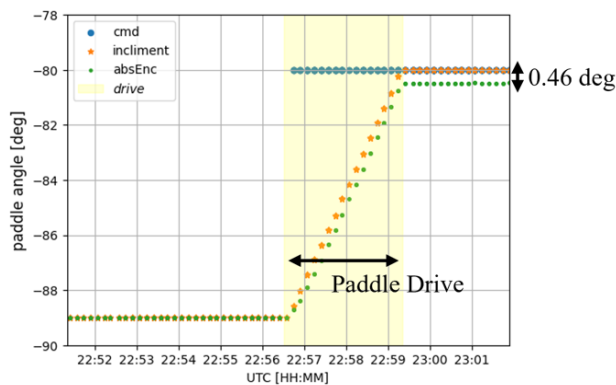


Fig 35. Paddle angle while paddle recovery

We conducted the paddle recovery operation while monitoring images and current flows to the motor every time. We consider unexpected phenomena like distortion of the paddle axis, driving the paddle every 10 degrees, and checking problems. We confirmed normally drive the paddle and now, the paddle angle returned to 0 degrees.

SUMMARY

We have developed and launched “HIBARI” to demonstrate a novel attitude control method called “Variable Shape Attitude Control (VSAC)” in 2021. We have achieved all minimum and full success, and now we have been operating the satellite to achieve extra success.

Through the operation of HIBARI, we learned about severe space environments such as Single Events of radiation and dealt with their degradation. Additionally, we faced problems that were unique to variable shape satellites and considered the resolve method.

1. Gyroscope anomalies on temperature and angular velocity.
2. Angle sensor degradation.

3. The output power of solar array paddle cells.
4. Sensor interference of drivable structures.
5. Drivable structure collided with the satellite bus from miss operation.

In the case of 1, One of its causes was assumed as the Single Event Effect. As countermeasures, we increased a sensor reset cycle. For the next satellite, we prepared gyroscope redundancy and designed a radiation shield. Regarding 2, The drivable structures are equipped outside the satellite, so the sensor is exposed to severe radiation. The sensor deteriorated and output anomalous values. As countermeasures, we will design a radiation shield and select radiation tolerant angle sensor for the next satellite. Regarding 3, We analyzed power generation of drivable solar array paddle cells. The output power of solar array paddle cells was low relative to ground tests. It is assumed that cell output power changes depending on environment such as thermal environment, satellite shape. As lessons, each drivable solar array paddle cell should input the power control unit separately. Regarding 4, There was sensor interference of drivable structures. The interference was caused by satellite shape change. We designed the satellite to avoid sensor interference by selecting sensor data, sensor arranging. However, some data indicates interfered data. For the next satellite, we need to make more suitable methods to select sensor data, sensor arrangement, and satellite shape design. Regarding 5, There was an accident that a drivable structure collided with the satellite bus from miss operation. We verified there was no fatal effect on the satellite system based on telemetry data and ground tests. And recovered normally checking satellite images by using a camera equipped with the satellite. Through this experience, we re-recognized the importance of the robust design of the satellite. These problems brought us precious experience and knowledge.

In the future, the Tokyo Institute of Technology (Institute of Science Tokyo) think about the next variable shape satellite. For example, formation flight using air-drag force, and solar sail using solar radiation pressure. Both are under consideration, we will develop next-generation variable shape satellites while utilizing HIBARI knowledge.

AKNOWLEDGEMENT

This work was supported by:

The Japan Society for the Promotion of Science
KAKENHI Grant Number JP17H01349 and
JP21H04588

Aerospace Commissioned Funds "Research and
Development Center for Smart Space Equipment and
Systems to Create a New Space Industry" of the Ministry
of Education, Culture, Sports, Science and Technology
(MEXT)

JST ERATO Grant Number JPMJER2102, Japan

We would like to appreciate the people who were
involved in JAXA's Innovative Satellite Technology
Demonstration Program 2, and the many people who
supported us in the development of HIBARI. We would
like to express our gratitude here.

REFERENCE

1. Watanabe, K., et al., "Concept Design and Development of 30kg Microsatellite HIBARI for Demonstration of Variable Shape Attitude Control," 33rd Annual AIAA/USU Conference on Small Satellites, SSC19-VII-02, Utah, U.S.A, 2019.
2. Watanabe, K., et al., "Engineering Model Development of HIBARI: MicroSatellite for Technology Demonstration of Variable-Shape Attitude Control," 34th Annual Small Satellite Conference, Utah, U.S.A, SSC20-V-07, 2020.
3. Watanabe, K., et al., "Flight Model Development and Ground Tests of Variable-Shape Attitude Control Demonstration MicroSatellite HIBARI," 33rd International Symposium on Space Technology and Science (ISTS), 2022-f-39, 2022.
4. Watanabe, K., et al., "Initial In-Orbit Operation Result of Microsatellite HIBARI: Attitude Control by Driving Solar Array Paddles," 36th Annual Small Satellite Conference, Utah, U.S.A, SSC22-WKII-05, 2022.
5. K. Yamada, "Attitude Control of Space Robot by Arm Motion," Journal of Guidance, Control, and Dynamics, Vol. 17, No. 5, 1994, pp. 1050-1054.
6. Tawara, K., Kikuya, Y., Kondo N., Yatsu, Y., and Matunaga, S., "Numerical Evaluation of On-Orbit Attitude Behavior for Microsatellites with Variable Shape Function," 67th International Astronautical Congress(IAC), Guadalajara, Mexico, 2016.
7. Watanabe, K., et al., "On-Orbit Performance Evaluation of Agile and Large-Angle Attitude Control of Spacecraft with Variable Shape Function," 34th International Symposium on Space Technology and Science (ISTS), 2023-f-04, 2023.
8. Hans, R., et al., "COTS for Space-Radiation Characterization of Gyro and IMUs for LEO Operations," 33th Annual Small Satellite Conference, Utah, U.S.A, SSC19-VII-01, 2019.